nature COMMUNICATIONS

ARTICLE

Received 20 Oct 2013 | Accepted 7 Jul 2014 | Published 8 Aug 2014

DOI: 10.1038/ncomms5601

Nuclear factor Y-mediated H3K27me3 demethylation of the *SOC1* locus orchestrates flowering responses of *Arabidopsis*

Xingliang Hou[1], Jiannan Zhou[2], Chang Liu[2], Lu Liu[2], Lisha Shen[2] & Hao Yu[2]

Nuclear factor Y (NF-Y) is a conserved heterotrimeric transcription factor complex that binds to the CCAAT motifs within the promoter region of many genes. In plants, a large number of genes code for variants of each NF-YA, B or C subunit that can assemble in a combinatorial fashion. Here, we report the discovery of an *Arabidopsis* NF-Y complex that exerts epigenetic control over flowering time by integrating environmental and developmental signals. We show that NF-Y interacts with CONSTANS in the photoperiod pathway and DELLAs in the gibberellin pathway, to directly regulate the transcription of *SOC1*, a major floral pathway integrator. This NF-Y complex binds to a unique *cis*-element within the *SOC1* promoter to modulate trimethylated H3K27 levels, partly through a H3K27 demethylase REF6. Our findings establish NF-Y complexes as critical mediators of epigenetic marks that regulate the response to environmental or intrinsic signals in plants.

[1] Key Laboratory of South China Agricultural Plant Molecular Analysis and Genetic Improvement, South China Botanical Garden, Chinese Academy of Sciences, Guangzhou, Guangdong 510650, China. [2] Department of Biological Sciences and Temasek Life Sciences Laboratory, National University of Singapore, Singapore 117543, Singapore. Correspondence and requests for materials should be addressed to X.H. (email: houxl@scib.ac.cn) or to H.Y. (email: dbsyuhao@nus.edu.sg).

The transition from vegetative to reproductive development is crucial for reproductive success of flowering plants. In *Arabidopsis*, the timing of this transition is controlled by a complex network of flowering genetic pathways in response to developmental cues and environmental signals[1]. The interactions among these flowering pathways regulate the expression of two floral pathway integrators, *FLOWERING LOCUS T* (*FT*) and *SUPPRESOR OF OVEREXPRESSION OF CONSTANS 1* (*SOC1*), which in turn activate the genes involved in the formation of floral meristems[2–5]. The major flowering pathways include photoperiod and gibberellin (GA) pathways that promote flowering in response to seasonal changes in day length and the endogenous phytohormone GA, respectively.

CONSTANS (CO) plays a central role in mediating photoperiod-dependent flowering[6]. When *CO* messenger RNA (mRNA) expression regulated by the circadian clock coincides with the exposure of plants to light under long days (LDs), the CO protein is stabilized in the nucleus and upregulates downstream genes, including *FT* and *SOC1*, to promote flowering[3,7,8]. Both CO in the photoperiod pathway and PHYTOCHROME INTERACTING FACTOR4 in the thermosensory pathway directly activate the mRNA expression of *FT* that encodes the protein as part of the florigen in leaves[3,9–11]. Long-distance movement of FT protein from leaves to the shoot apex through the phloem system allows FT to interact with a bZIP transcription factor FD in the shoot apical meristem for activating floral meristem identity genes[10,12,13]. *SOC1* is expressed in leaves and shoot apical meristems in response to multiple flowering pathways, and encodes a MADS-box transcription factor that acts as a key flowering promoter through regulating another floral meristem identity gene, *LEAFY*[2–5,14–16]. Although several studies indicate that CO activates *SOC1* either directly or indirectly via FT in the photoperiod pathway[3,10,17,18], so far there is no evidence to support direct regulation of *SOC1* transcription by CO or FT.

The GA pathway also plays an important role in the promotion of flowering in *Arabidopsis* under both LDs and short days, although its effect under LDs is usually masked by the photoperiod pathway[19,20]. Molecular genetic analyses of GA and photoperiod pathways suggest that the photoperiod and GA pathways are coordinated to promote flowering under LDs[15,20,21]. The GA effect on flowering is genetically mediated by five DELLA proteins, GIBBERELLIC ACID INSENSITIVE (GAI), REPRESSOR OF *ga1-3* (RGA), RGA-LIKE1 (RGL1), RGL2 and RGL3, which are key GA signalling repressors whose degradation is triggered by GA[22,23]. As transcriptional regulators, DELLA proteins have been shown to exert their function by recruiting other transcription factors rather than directly binding to their target genes[24–27].

It has been suggested that photoperiod-dependent flowering involves nuclear factor Y (NF-Y) complexes, which are conserved combinatorial transcription factors in eukaryotes consisting of NF-YA, NF-YB and NF-YC subunits[28–32]. NF-Y and its binding element, the CCAAT box, are among the first set of *trans*-acting factors and *cis*-elements identified in eukaryotes[33]. The *Arabidopsis* genome contains 10 NF-YA, 13 NF-YB and 13 NF-YC subunits, which could theoretically form 1,690 unique heterotrimeric NF-Y transcription factors, potentially enabling the specific control of a variety of target genes[32,34]. In this study, we report the discovery of a complete NF-Y complex consisting of three different subunits that regulates flowering time in response to photoperiod and GA pathways in *Arabidopsis*. NF-Y subunits interact with CO and DELLAs to directly regulate *SOC1* expression. The NF-Y complex binds to a unique *cis*-element in the *SOC1* promoter through its NF-YA2 subunit, and modulates H3K27me3 dynamics at *SOC1* partly via RELATIVE OF EARLY FLOWERING 6 (REF6), a H3K27 demethylase. Our findings uncover that the combinatorial NF-Y transcription factor plays a critical role in mediating epigenetic control of the floral transition through its interaction with key regulators in the photoperiod and GA pathways, thus orchestrating plant responses to environmental and intrinsic flowering signals.

Results

DELLAs and CO interact with NF-Y subunits. DELLA proteins function as key transcriptional regulators that mediate GA effect on plant development. To further investigate the function of DELLA proteins, we performed a yeast two-hybrid screening to identify RGA-interacting partners using an inflorescence cDNA library (CD4-30 from ABRC)[26], and found that RGA interacted with NF-YC3 and its closest homologue NF-YC9, two *Arabidopsis* NF-YC family members[32,34], in yeast. This result, together with a recent finding describing the involvement of NF-YC3 and NF-YC9 in CO-mediated control of flowering[28], prompted us to investigate whether DELLAs and CO coordinately interact with NF-Y subunits to regulate flowering time.

To systematically study the protein interactions of representative NF-Y subunits with RGA and CO, we selected two NF-YA (A1 and A2), three NF-YB (B1, B2 and B3), and three NF-YC (C1, C3 and C9) homologues because they are either relevant with flowering time control or expressed in the vasculature similarly to *CO*[28–31,34]. Yeast two-hybrid assays revealed that in addition to NF-YC3 and NF-YC9 found in initial yeast two-hybrid screening, RGA also interacted strongly with NF-YA1 and NF-YA2, and weakly with NF-YB2 (Fig. 1a). CO not only interacted with all NF-YC subunits examined, but also interacted weakly with NF-YB2 (Fig. 1a). Glutathione S-transferase (GST) pull-down assays verified the protein interactions of the selected NF-YB and NF-YC subunits (NF-YB2 and NF-YC9) with RGA and CO, but did not show the interaction between RGA and the selected NF-YA subunit (NF-YA2) (Fig. 1b) as revealed by yeast two-hybrid assays. We further performed bimolecular fluorescence complementation (BiFC) analyses, and found the interactions of all selected NF-Y subunits (NF-YA2, NF-YB2 and NF-YC9) with RGA and CO in the nuclei of tobacco cells (Fig. 1c, Supplementary Fig. 1). Therefore, these results consistently demonstrate that RGA and CO interact with NF-YB and NF-YC subunits, while the interaction of NF-YA subunits with RGA and CO may depend on other endogenous factors in plants, such as NF-YC subunits, as discussed later.

To test whether the selected NF-Y subunits that interact with RGA and CO could form heterotrimeric NF-Y transcription factors, we performed yeast two-hybrid assays to examine the interactions among these NF-Y subunits. NF-YC3 and NF-YC9 interacted with both NF-YA and NF-YB subunits (Supplementary Fig. 2), whereas no interactions between NF-YA and NF-YB subunits were observed (Fig. 1d, upper panel). Yeast three-hybrid assays further showed that NF-YC9 was required for the interactions between NF-YA and NF-YB subunits (Fig. 1d). BiFC analysis confirmed the interactions of NF-YC9 with NF-YA2 and NF-YB2 in the nuclei of tobacco cells (Fig. 1c). These results, together with a recent study on the bilateral interactions between NF-Y subunits[35], suggest that NF-YC subunits directly interact with NF-YA and NF-YB subunits, and might be necessary for the interaction between NF-YA and NF-YB subunits for the assembly of the trimeric NF-Y complex.

As NF-YC9 interacted with other NF-Y subunits, RGA and CO in yeast and tobacco cells (Fig. 1a,c, Supplementary Fig. 2), we created *pNF-YC9:NF-YC9-FLAG* plants to examine the interaction of NF–YC9 with other proteins in *Arabidopsis*. *pNF-YC9:NF-*

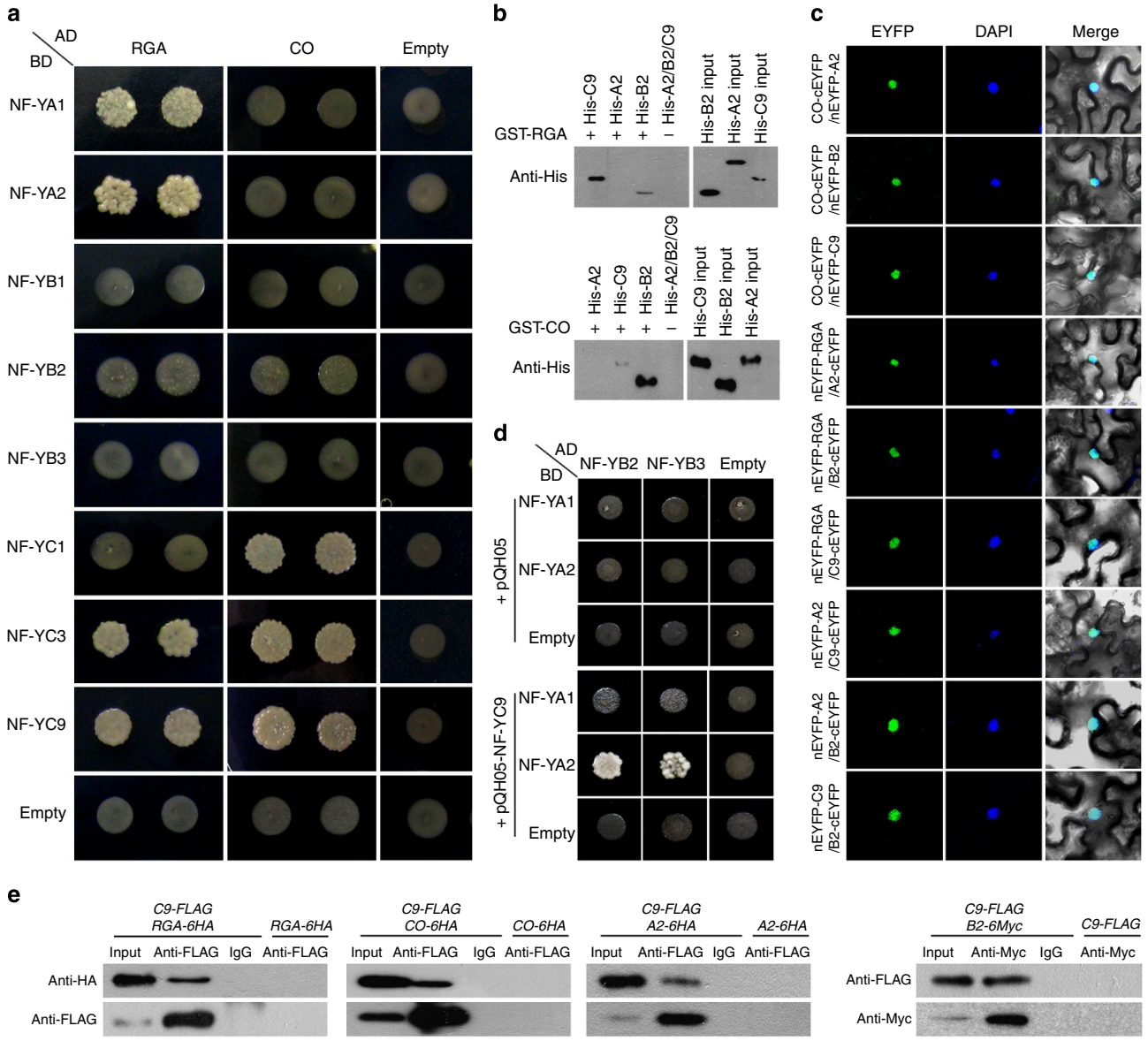

Figure 1 | CO and RGA interact with NF-Y subunits *in vitro* and *in vivo*. (**a**) Yeast two-hybrid assays show the interactions of NF-Y subunits with RGA and CO. Transformed yeast cells were grown on SD-Trp/-Leu/-His/-Ade medium. (**b**) *In vitro* pull-down assays show the interactions of NF-Y subunits with RGA and CO. His-tagged proteins were incubated with immobilized GST (−) or GST-tagged proteins (+) and immunoprecipitated fractions were detected by anti-His antibody. (**c**) BiFC analysis of the interactions among NF-Y subunits and between NF-Y subunits and CO or RGA in tobacco epidermal cells. Enhanced yellow fluorescence protein (EYFP), fluorescence of enhanced yellow fluorescent protein; DAPI, fluorescence of 4′,6-diamino-2-phenylindol; Merge, merge of EYFP, DAPI and bright field. (**d**) Yeast three-hybrid assays show the interactions between NF-YA and NF-YB subunits in the presence of NF-YC9. The empty vector pQH05 was co-transformed with AD and BD plasmids to serve as a control in the upper panel. Transformed yeast cells were grown on SD-Trp/-Leu/-His/-Ade medium. (**e**) *In vivo* interaction among NF-Y subunits and between NF-YC9 and CO or RGA in *Arabidopsis*. Plant nuclear extracts from various 9-day-old transgenic seedlings grown under LDs were immunoprecipitated by anti-Myc antibody, anti-FLAG antibody or preimmune serum (IgG) as indicated above each blot. The co-immunoprecipitated proteins were detected by anti-FLAG, anti-Myc or anti-HA antibody as indicated on the left of the blots. *C9-FLAG, nf-yc9-1 pNF-YC9:NF-YC9-FLAG; RGA-6HA, ga1-3 35S:RGA-6HA; CO-6HA, SUC2:CO-6HA; A2-6HA, 35S:NF-YA2-6HA; B2-6Myc, pNF-YB2:NF-YB2-6Myc.*

YC9-FLAG rescued the late-flowering phenotype of *nf-yc3-2 nf-yc4-1 nf-yc9-1* (ref. 28) (Table 1), indicating that NF-YC9-FLAG retains the biological function of NF-YC9. The *nf-yc9-1 pNF-YC9:NF-YC9-FLAG* line was crossed with various plants containing other tagged transgenes and the resulting homozygous progenies were used for co-immunoprecipitation analyses. Our results revealed the *in vivo* interaction of NF-YC9 with RGA, CO, NF-YA2 and NF-YB2 (Fig. 1e, Supplementary Fig. 3). Taken together, these data suggest that RGA and CO interact with NF-Y subunits, and that NF-YC9 is a common partner interacting with other proteins involved. Similar to RGA, other DELLA proteins, such as GAI, RGL1 and RGL2, also interacted with NF-Y subunits (Supplementary Fig. 4), implying widespread interactions between DELLAs and NF-Y.

Interactions among CO, GA signalling and NF-Y. Because previous studies have shown that CO, GA signalling, and

Table 1 | Flowering time of various plants in this study.

Genotype	No. of rosette leaves	No. of cauline leaves	No. of days to flowering
Experiment 1 (LDs)			
Col	12.2 ± 0.5	3.8 ± 0.3	26.5 ± 0.5
soc1-2	21.4 ± 0.8	5.2 ± 1.3	40.5 ± 1.6
co-1	18.4 ± 0.4	5.1 ± 0.5	35.4 ± 1.2
ga1	18.5 ± 1.2	ND	36.0 ± 2.0
co-1 ga1	Hardly flowering	ND	ND
co-1 ga1 rga28	20.3 ± 1.8	ND	38.5 ± 1.2
nf-ya2-1	12.8 ± 0.4	4.0 ± 0.3	26.8 ± 0.3
nf-yb2-1	14.7 ± 0.2	4.2 ± 0.2	32.0 ± 0.5
nf-yb3-1	14.8 ± 0.3	4.2 ± 0.1	31.5 ± 0.4
nf-yc3-2	11.3 ± 0.5	3.2 ± 0.1	25.8 ± 0.4
nf-yc4-1	12.6 ± 0.4	3.8 ± 0.2	26.5 ± 0.6
nf-yc9-1	12.5 ± 0.4	3.6 ± 0.2	26.2 ± 0.3
nf-yb2-1 nf-yb3-1	23.0 ± 0.8	8.0 ± 0.8	43.5 ± 0.8
nf-ya2-1 nf-yc9-1	13.1 ± 0.6	4.0 ± 0.4	27.2 ± 0.5
nf-ya2-1 nf-yb2-1 nf-yb3-1 nf-yc9-1	27.5 ± 1.2	9.1 ± 0.3	49.7 ± 2.4
nf-yc3-2 nf-yc4-1 nf-yc9-1	21.1 ± 0.5	7.8 ± 0.4	39.4 ± 0.5
nf-yb2-1 nf-yb3-1 co-1	23.2 ± 0.7	9.3 ± 0.2	45.1 ± 0.5
nf-yb2-1 nf-yb3-1 ga1	Hardly flowering	ND	ND
35S:CO (Col)	5.0 ± 0.2	3.1 ± 0.1	11.0 ± 0.5
ga1 35S:CO (Col)	5.2 ± 0.2	ND	11.2 ± 1.0
SUC2:CO-6HA	4.5 ± 0.3	2.8 ± 0.2	10.8 ± 0.3
nf-yb2-1 nf-yb3-1 SUC2:CO-6HA	20.5 ± 2.3	6.2 ± 1.0	37.8 ± 2.0
Experiment 2 (LDs)			
Ler	7.9 ± 0.3	4.0 ± 0.2	21.4 ± 0.2
co-2	15.3 ± 0.6	6.0 ± 0.5	35.5 ± 1.5
ga1-3	8.8 ± 0.5	N.D.	22.5 ± 0.3
ga1-3 gai-t6 rga-t2	8.0 ± 0.2	4.2 ± 0.4	21.0 ± 0.5
co-2 ga1-3	Hardly flowering	ND	ND
co-2 ga1-3 gai-t6 rga-t2	11.5 ± 0.7	6.3 ± 0.6	28.4 ± 0.6
gai-t6 rga-t2	7.1 ± 0.2	4.2 ± 0.1	20.0 ± 0.4
co-2 gai-t6 rga-t2	11.2 ± 0.4	6.0 ± 0.5	27.1 ± 0.3
gai-t6 rga-t2 rgl1-1 rgl2-1	5.8 ± 0.3	3.2 ± 0.2	18.2 ± 0.4
co-2 gai-t6 rga-t2 rgl1-1 rgl2-1	6.9 ± 0.6	3.5 ± 0.5	19.5 ± 0.3
35S:CO (Ler)	3.2 ± 0.2	2.8 ± 0.2	11.0 ± 0.2
ga1-3 35S:CO (Ler)	3.4 ± 0.3	ND	11.2 ± 0.2
Experiment 3 (LDs)			
Col	12.5 ± 0.3	3.7 ± 0.5	26.3 ± 0.6
nf-yb2-1	15.2 ± 0.2	4.5 ± 0.2	32.2 ± 0.5
nf-yb2-1 pNF-YB2:NF-YB2-6Myc	12.4 ± 0.3	4.0 ± 0.3	27.1 ± 0.5
nf-yc3-2 nf-yc4-1 nf-yc9-1	21.5 ± 0.4	7.8 ± 0.3	39.6 ± 0.7
nf-yc3-2 nf-yc4-1 nf-yc9-1	13.0 ± 0.4	3.8 ± 0.5	27.5 ± 0.5
pNF-YC9:NF-YC9-FLAG			
35S:NF-YC9-6HA	10.5 ± 0.3	3.5 ± 0.2	25.0 ± 0.5
35S:NF-YC3-6HA	12.1 ± 0.4	4.0 ± 0.3	26.5 ± 0.8
35S:NF-YA2-6HA	11.0 ± 0.4	3.7 ± 0.4	25.4 ± 0.5
Experiment 4 (LDs)			
Col	12.4 ± 0.3	3.9 ± 0.2	26.6 ± 0.4
co-1	18.5 ± 0.6	5.0 ± 0.3	35.5 ± 1.0
ga1	18.8 ± 0.9	ND	36.2 ± 1.8
nf-yb2-1 nf-yb3-1	23.3 ± 0.7	8.1 ± 0.6	43.4 ± 1.1
clf	9.1 ± 0.8	3.0 ± 0.0	23.2 ± 0.2
ref6-1	14.4 ± 0.8	4.8 ± 0.6	30.5 ± 0.4
REF6ox	2.5 ± 0.5	1.8 ± 0.3	18.0 ± 0.6
co-1 REF6ox	2.8 ± 0.7	2.5 ± 0.5	18.0 ± 0.5
ga1 REF6ox	7.8 ± 0.6	ND	20.5 ± 1.5
nf-yb2-1 nf-yb3-1 ref6-1	32.7 ± 0.5	9.3 ± 0.8	51.8 ± 1.8
nf-yb2-1 nf-yb3-1 ref6-1 pREF6:REF6-HA	23.8 ± 0.8	8.5 ± 0.5	45.5 ± 2.1
nf-yb2-1 nf-yb3-1 REF6ox	12.5 ± 0.5	3.5 ± 0.5	28.5 ± 1.2
Experiment 5 (SDs)			
Col	45.6 ± 2.1	8.0 ± 1.0	84.5 ± 2.5
nf-yb2-1 nf-yb3-1	48.4 ± 2.8	8.1 ± 0.6	95.6 ± 2.3
nf-ya2-1 nf-yb2-1 nf-yb3-1 nf-yc9-1	61.5 ± 2.7	9.8 ± 0.6	111.7 ± 3.4

LDs, long days; SDs, short days.
Flowering time is presented as the number of rosette and cauline leaves formed on the main shoot, and the days from sowing to flowering. Values are mean ± s.d. from at least 20 plants for each genotype.
ND, results could not be determined because plants either do not flower or flower without bolting during our experimental period.

individual NF-YB/C subunits are all involved in the control of flowering time under LDs[20,21,28–31], we proceeded to study how their interactions affect flowering. We first crossed *nf-ya2-1* and *nf-yc9-1* (ref. 28) with *nf-yb2-1 nf-yb3-1* that showed late flowering[30]. The resulting quadruple mutant *nf-ya2-1 nf-yb2-1 nf-yb3-1 nf-yc9-1* exhibited even later flowering (Table 1), indicating that the heterotrimeric complex of the NF-Y transcription factor comprising YA, YB and YC subunits play an important role in determining flowering time.

As NF-Y subunits interacted *in vivo* with RGA and CO (Fig. 1), we hypothesized that they could coordinately regulate certain common targets in both photoperiod and GA pathways. Thus, we tested the temporal expression of *SOC1* and *FT*, both of which act downstream of photoperiod and GA pathways. Both *SOC1* and *FT* were consistently downregulated in *co-1*, the GA-deficient mutant *ga1*, *nf-yb2-1 nf-yb3-1*, and *nf-ya2-1 nf-yb2-1 nf-yb3-1 nf-yc9-1* during the floral transition, whereas there was no consistent change in *CO* expression in these mutants (Fig. 2a). Furthermore, induced CO activity upregulated *SOC1* and *FT* in a steroid-inducible *co-2 35S:CO-GR* line as previously reported[3] (Fig. 2b, Supplementary Fig. 5). Similarly, induced RGA activity downregulated *SOC1* and *FT* in a steroid-inducible *35S:RGA-GR* line[36] in the background of *ga1-3 gai-t6 rga-t2* (Fig. 2b, Supplementary Fig. 5), in which null mutants of RGA and GAI, two major DELLA proteins mediating GA effect on flowering, suppressed the non-flowering defect of *ga1-3* (ref. 22). These results demonstrate that CO, GA signalling and NF-Y all affect *SOC1* and *FT* expression under LDs.

We then investigated genetic interactions among CO, GA signalling and NF-Y. Consistent with the role of CO in the promotion of flowering, *co-1* showed late flowering, while *SUC2:CO-6HA* showed early flowering (Fig. 2c, Table 1, Supplementary Fig. 6). *nf-yb2-1 nf-yb3-1* exhibited the comparable late-flowering phenotype to *nf-yb2-1 nf-yb3-1 co-1*, and almost completely suppressed early flowering of *SUC2:CO-6HA* (Fig. 2c, Supplementary Fig. 6, Table 1). Consistently, upregulation of *SOC1* and *FT* expression in *SUC2:CO-6HA* was greatly attenuated in a *nf-yb2-1 nf-yb3-1* background (Supplementary Fig. 6). These results suggest that NF-Y predominantly mediates CO effect on downstream flowering promoters. In contrast, *ga1* (Columbia (Col) background) and *ga1-3* (Landsberg *erecta (Ler* background)), both of which exhibited late flowering to different extents, did not affect early flowering of overexpression of *CO* (Fig. 2d, Table 1). Furthermore, both *co-1 ga1* (Col background) and *co-2 ga1-3* (*Ler* background) hardly flowered under our experimental period (Fig. 2e, Table 1). These results support that CO and GA signalling partially function in parallel pathways to control flowering under LDs. Since CO controlled flowering in a NF-Y-dependent manner, *nf-yb2-1 nf-yb3-1 ga1* expectedly exhibited the non-flowering defect similar to *co-1 ga1* under LDs (Fig. 2f, Table 1).

NF-Y subunits are associated with the *SOC1* promoter. The interaction of NF-Y subunits with RGA and CO and their effects on *SOC1* and *FT* expression provoked us to speculate whether NF-Y serves as a convergent point to mediate flowering through

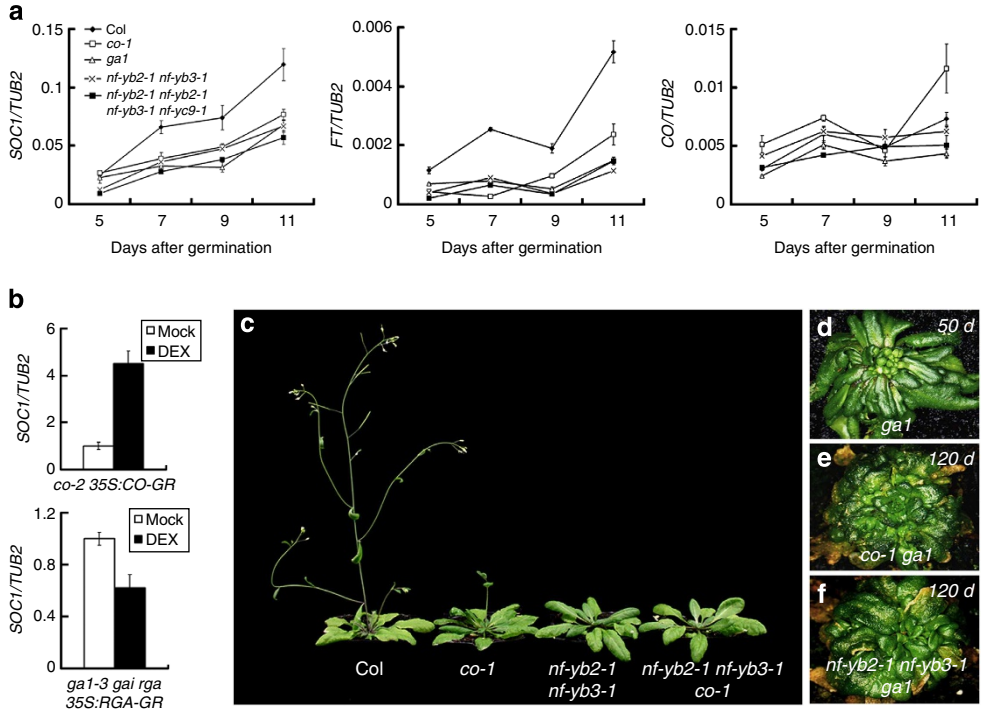

Figure 2 | CO, GA signalling and NF-Y regulate flowering. (**a**) Quantitative RT–PCR analysis of temporal expression of *SOC1*, *FT* and *CO* in developing seedlings with various genetic backgrounds under LDs. The β-tubulin gene (*TUB2*) was amplified as an internal control. Values are mean ± s.d. of three biological replicates. (**b**) *SOC1* expression in *co-2 35S:CO-GR* and *ga1-3 gai-t6 rga-t2 35S:RGA-GR* seedlings. Seven-day-old seedlings grown under LDs were either mock treated or treated with 10 μM dexamethasone (DEX) for 4 h. *SOC1* expression was calculated by comparing the value of DEX treatment to that of mock treatment. Values are mean ± s.d. of three biological replicates. (**c**) *nf-yb2-1 nf-yb3-1 co-1* exhibits comparable flowering time to *nf-yb2-1 nf-yb3-1*. Flowering phenotypes of representative 32-day-old plants with various genetic backgrounds grown under LDs were compared. (**d**–**f**) *co-1 ga1* and *nf-yb2-1nf-yb3-1 ga1* hardly flower as compared with *ga1*. Flowering phenotypes of 50-day-old *ga1* (**d**), 120-day-old *co-1 ga1* (**e**) and 120-day-old *nf-yb2-1 nf-yb3-1 ga1* (**f**) grown under LDs were compared. Note that 50-day-old *ga1* has generated floral buds (**d**), whereas *co-1 ga1* (**e**) and *nf-yb2-1 nf-yb3-1 ga1* (**f**) do not flower within our experimental period.

regulating *SOC1* and *FT* expression in response to both photoperiod and GA pathways. To this end, we first examined whether NF-Y subunits are directly associated with *SOC1* and *FT* regulatory regions. Chromatin immunoprecipitation (ChIP) assays of *nf-yc9-1 pNF-YC9:NF-YC9-FLAG* and *nf-yb2-1 pNF-YB2:NF-YB2-6Myc* in which *pNF-YB2:NF-YB2-6Myc* rescued the late-flowering phenotype of *nf-yb2-1* (Table 1) revealed that both NF-YC9-FLAG and NF-YB2-6Myc were associated with the genomic region near the *SOC1-5* fragment with the highest enrichment fold (Fig. 3a). We further created *35S:NF-YA2-6HA*, *35S:NF-YC3-6HA* and *35S:NF-YC9-6HA* transgenic plants, all of which showed slightly early flowering and dwarf or semi-dwarf stature (Supplementary Fig. 7, Table 1), indicating that these NF-Y subunits mediate similar developmental processes. ChIP assays of these materials demonstrated that these NF-Y subunits tagged with 6HA bound to the same *SOC1* genomic region as NF-YC9-FLAG and NF-YB2-6Myc (Fig. 3a, Supplementary Fig. 8). These results and the observation on the interactions among these NF-Y subunits suggest that three different types of subunits form the heterotrimeric NF-Y complex that recognizes the same binding region in the *SOC1* promoter.

We further tested whether CO and RGA also bind to *SOC1* by ChIP analysis of *SUC2:CO-6HA* and *ga1-3 gai-t6 rgl1-1 rgl2-1 rga-t2 35S:RGA-6HA*[37]. Association of CO-6HA with *SOC1* spanned a ~1.7 kb promoter region from *SOC1-1* to *SOC1-9* fragments with an enrichment peak at around *SOC1-7* (Fig. 3a). In contrast, association of RGA-6HA with the *SOC1* genomic region was not detectable (Supplementary Fig. 8). These observations imply that CO and NF-Y co-localize at the *SOC1* promoter, whereas the interaction between RGA and NF-Y could be separate from NF-Y association with the *SOC1* promoter.

Notably, although ChIP analysis of *SUC2:CO-6HA* revealed the association of CO-6HA with a 9-kb *FT* genomic region with an enrichment peak at the *FT-14* fragment, there was no significant enrichment detectable for NF-YA2, NF-YB2, and NF-YC9 (Supplementary Fig. 9). Thus, these NF-Y subunits might affect *FT* expression in an indirect manner.

The association of CO-6HA with both *SOC1* and *FT* genomic regions implies that CO could directly regulate both genes as previously suggested[3,18]. This is supported by additive effects of *ft soc1* mutants on delaying flowering under LDs[17,38]. We also found that *SOC1* was significantly upregulated in *ft-10 SUC2:CO-6HA* compared with *ft-10* (Supplementary Fig. 10). This result, together with the ChIP result showing direct binding of CO to *SOC1*, suggests that CO partially activates *SOC1* expression independently of FT.

NF-YA2 directly binds to the NFYBE of the *SOC1* promoter. To identify the subunit(s) of the NF-Y complex that interacts with the *SOC1-5* fragment, we performed the electrophoretic mobility shift assay (EMSA) using the biotinylated *SOC1-5* fragment as a probe, and found that only NF-YA2 specifically bound to *SOC1-5* (Supplementary Figs 11 and 12). This is consistent with a previous study showing that only NF-YA subunits contain the essential histidine residues required for NF-Y binding to DNA[39].

We further revealed that NF-YA2 only bound to the middle subfragment of *SOC1*-5 that contains a 15-bp motif flanked by a pair of inverted repeat sequences (Supplementary Figs 11 and 13), which could facilitate the protein-DNA interaction[40]. We then performed EMSA using this 15-bp motif and its mutated versions as probes, and found that NF-YA2 bound to the native motif rather than the mutated version (*Mut1*) (Fig. 3b,c). This motif (5′-TTCACAAACACCATT-3′) was, thus, designated as the NFYBE.

NF-Y binding mediates the regulation of *SOC1* by CO and GA. To test *in vivo* whether CO and GA signalling regulate *SOC1* through NF-Y binding to the NFYBE in the *SOC1* promoter, we used an established *pSOC1:β-glucuronidase* (*GUS*) construct in which the *GUS* reporter gene was driven by a 2-kb *SOC1* promoter upstream of the translational start site[5]. Based on this construct, we further created a mutated reporter gene cassette containing the *Mut1* version of the NFYBE, 5′-TTCAgtAAgACgATT-3′ (Fig. 3b). Among 30 lines of transformants harbouring the mutated version, 28 lines displayed significantly reduced GUS staining at 4 and 9 days after germination compared with *pSOC1:GUS* plants (Fig. 3d,e), suggesting that the NFYBE is critical for promoting *SOC1* expression during the floral transition.

We then crossed the representative native and mutated *pSOC1:GUS* plants with *nf-yb2-1 nf-yb3-1* and *35S:CO*. GUS staining of *pSOC1:GUS* was significantly weaker in both 4- and 9-day-old *nf-yb2-1 nf-yb3-1* seedlings than that in wild-type seedlings, whereas there was no significant difference in the intensity of GUS staining for the mutated *pSOC1:GUS* in two different genetic backgrounds (Fig. 3d,e). Thus, mutagenesis of the NFYBE abolishes NF-Y capacity in upregulating *SOC1*, confirming that NF-Y promotes *SOC1* expression through binding to the NFYBE. As expected, *pSOC1:GUS* displayed increased GUS staining in *35S:CO* compared with wild-type seedlings, but the mutated *pSOC1:GUS* displayed the same weak staining in both *35S:CO* and wild-type backgrounds (Fig. 3d,e). Furthermore, GA treatment resulted in increased GUS staining in 9-day-old *pSOC1:GUS* seedlings compared with non-treated seedlings, but had no effect on the mutated *pSOC1:GUS* seedlings.

To directly test whether the NFYBE affects flowering, we transformed a 6.6-kb native *SOC1* genomic fragment and its

Figure 3 | CO and GA signalling regulate *SOC1* expression through NF-Y binding to the *SOC1* promoter. (**a**) ChIP analysis of binding of NF-Y subunits and CO to the *SOC1* regulatory regions. Nine-day-old seedlings grown under LDs were collected for ChIP analysis. Fifteen DNA fragments spanning the *SOC1* genomic region shown in Supplementary Fig. 8 were examined by ChIP-enrichment test. Values are mean ± s.d. of three biological replicates. (**b**) List of the putative NF-YA2 binding element (*Native*) in *SOC1-5* fragment and its mutated versions (*Mut1-5*) used for EMSA assays shown in **c**. (**c**) EMSA assay of the sequence elements required for NF-YA2 binding to *SOC1*. The biotinylated native probe was added in the absence (−) or the presence of 1 μg purified His-NF-YA2 protein (+). Various non-labelled probes (cold competitors) in 10- and 50-fold molar excess relative to the biotinylated native probe were used as competitors. *SOC1-5* fragment (Supplementary Fig. 11) serves as a positive control. Arrow indicates the specific binding of NF-YA2 protein to the biotinylated native probe, while arrowhead indicates non-specific bands. (**d**) Representative GUS staining of 4-day-old (upper panels) and 9-day-old (lower panels) seedlings containing *pSOC1:GUS* (Native) and its mutated construct (Mutated) in various genetic backgrounds. Seeds were germinated and grown on either MS medium or MS medium containing 10 μM GA_3 for the GA treatment experiment. (**e**) Quantitative analysis of GUS activity in various *pSOC1:GUS* plants shown in (**d**). Values were mean ± s.d. from at least 30 plants of each genotype or treatment. Asterisks indicate significant changes in GUS activity in comparison with respective controls (two-tailed Student's *t*-test, $P<0.05$). There is no statistically significant difference in GUS activity among plants containing the mutated *pSOC1:GUS* construct in various genetic backgrounds. (**f**) Distribution of flowering time in T1 transgenic plants containing a 6.6-kb *SOC1* genomic fragment (*native gSOC1*) and its derived version with the mutated NFYBE (*mutated gSOC1*) in the *soc1-2* mutant background.

derived version with the mutated NFYBE into *soc1-2*. Most of the independent *soc1-2* lines transformed with the native fragment exhibited comparable flowering time as wild-type plants, whereas almost all the *soc1-2* lines transformed with the mutated version flowered later than wild-type plants (Fig. 3f), demonstrating that mutagenesis of the NFYBE compromises the *SOC1* effect on promoting flowering. Taken together, these observations strongly support that NF-Y binding to the NFYBE partly contributes to

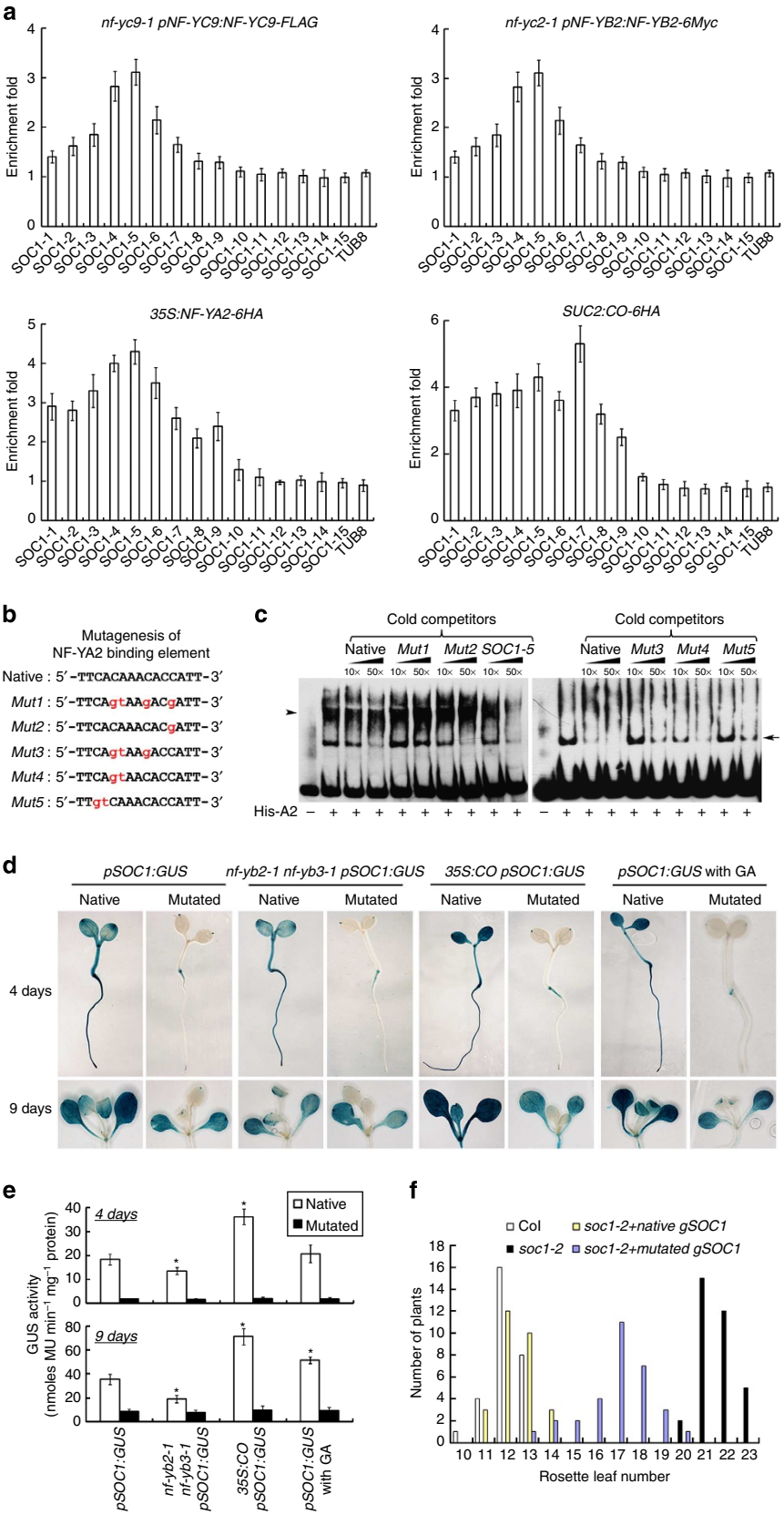

the upregulation of *SOC1* in response to CO and GA signalling during the floral transition.

GA signalling enhances NF-Y binding to the *SOC1* promoter. As our genetic analyses suggest that CO and GA signalling function in parallel pathways to control flowering under LDs (Fig. 2e, Table 1), we then investigated the relative contribution of GA and CO to modulating flowering. GA treatment accelerated flowering of wild-type plants in both Col and L*er* backgrounds under LDs (Supplementary Table 1). Consistently, GA-deficient mutants, *ga1-3* (L*er* background) and *ga1* (Col background), exhibited late flowering, while loss of function of DELLA proteins in *gai-t6 rga-t2 rgl1-1 rgl2-1* exhibited early flowering (Fig. 4a, Table 1). These data demonstrate that GA signalling contributes to the promotion of flowering under LDs even when the photoperiod pathway mediated by CO plays a dominant role. However, in the absence of CO, the fundamental effect of GA on flowering under LDs was clearly perceived as evident from the observations that GA treatment greatly accelerated flowering of *co-1*, *co-2* and *co-1 ga1* (Supplementary Table 1), and that *gai-t6 rga-t2 rgl1-1 rgl2-1* or *gai-t6 rga-t2* fully rescued the late-flowering phenotype of *co-2* or the non-flowering phenotype of *co-2 ga1-3* (Fig. 4a, Table 1). Furthermore, *SOC1* and *FT* expression was upregulated in *gai-t6 rga-t2 rgl1-1 rgl2* regardless of CO activity (Fig. 4b). These observations support that GA signalling directly modulates flowering regulators, such as *SOC1*, in parallel to CO.

Although both CO and RGA interacted with NF-Y subunits (Fig. 1) and regulated *SOC1* expression through NF-Y binding to *SOC1* (Fig. 3b–e), the *SOC1* promoter was only associated with CO and NF-Y, but not RGA (Fig. 3a, Supplementary Fig. 8). To understand how the interaction between RGA and NF-Y regulates *SOC1* expression, we first examined whether treatment of GA or an inhibitor of GA biosynthesis, paclobutrazol (PAC), affects the protein levels of NF-YC9 that interacted *in vivo* with RGA (Fig. 1e). Neither GA treatment that degraded DELLA proteins including RGA nor PAC treatment that stabilized DELLA proteins affected the abundance of NF-YC9-FLAG in *nf-yc9-1 pNF-YC9:NF-YC9-FLAG* (Fig. 4c). However, ChIP assays of *nf-yc9-1 pNF-YC9:NF-YC9-FLAG* revealed that NF-YC9-FLAG binding to the *SOC1* promoter was significantly enhanced or compromised by GA or PAC treatment, respectively (Fig. 4d). Thus, GA signalling regulates flowering through enhancing NF-Y binding to *SOC1* rather than affecting the expression levels of NF-Y proteins.

NF-Y reduces H3K27me3 levels at *SOC1*. Although several studies have correlated NF-Y binding to histone marks at downstream genes[41–43], it is so far unclear whether NF-Y affects histone modifications in plants. To understand how NF-Y regulates *SOC1* transcription, we compared the distribution profiles of several selected histone marks, including H3ac, H4ac, H3K4me2, H3K4me3, H3K9ac and H3K27me3, at the *SOC1* locus between wild-type and *nf-ya2-1 nf-yb2-1 nf-yb3-1 nf-yc9-1* plants by ChIP assays. While these histone marks were all enriched to different extents at *SOC1*, H3K27me3 exhibited the most dramatic change in its levels in *nf-ya2-1 nf-yb2-1 nf-yb3-1 nf-yc9-1* as compared with wild-type plants (Fig. 5a, Supplementary Fig. 14). H3K27me3 is a histone mark associated with transcriptionally silent chromatin, which is specifically recognized by TERMINAL FLOWER 2 (TFL2), the only *Arabidopsis* homologue of HP1 (ref. 44). ChIP analysis using *tfl2-1 35S:TFL2-3HA*[45] showed the association of TFL2-3HA with *SOC1* at the same region (*SOC1-10*) highly enriched for H3K27me3 (Fig. 5a,b), confirming the deposition of H3K27me3 at *SOC1*. The progressive increase of H3K27me3 levels at *SOC1* in *nf-yb2-1 nf-yb3-1* and *nf-ya2-1 nf-yb2-1 nf-yb3-1 nf-yc9-1*

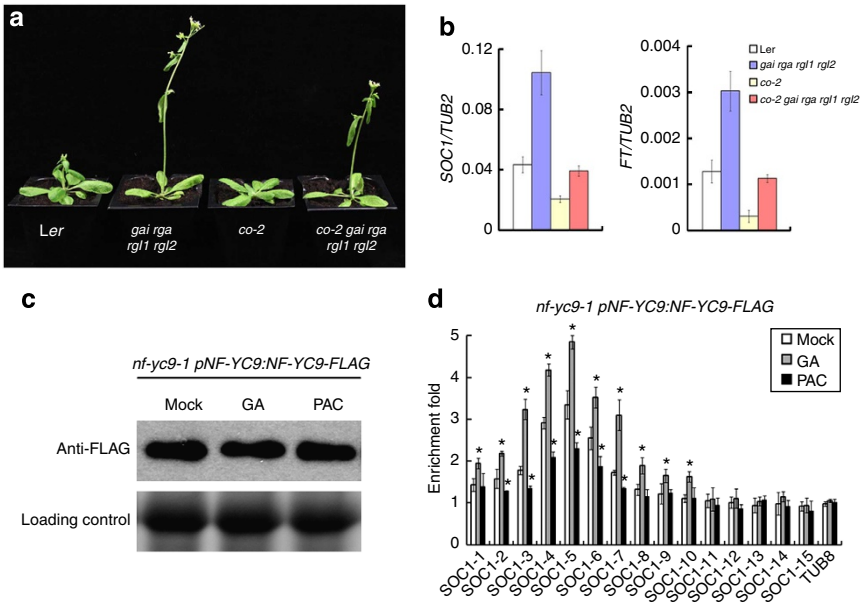

Figure 4 | GA signalling promotes *SOC1* through enhancing NF-Y binding to the *SOC1* promoter. (**a**) Loss of function of DELLAs accelerates flowering in both wild-type and *co-2* plants. Flowering phenotypes of representative 23-day-old plants with various genetic backgrounds grown under LDs were compared. (**b**) Quantitative RT–PCR analysis of *SOC1* and *FT* expression in 7-day-old seedlings with various genetic backgrounds under LDs. *TUB2* was amplified as an internal control. Values are mean ± s.d. of three biological replicates. (**c**) Western blot analysis of NF-YC9-FLAG expression in total protein extract from 9-day-old *nf-yc9-1 pNF-YC9:NF-YC9-FLAG* plants mock treated or treated with 100 μM GA_3 or 10 μM PAC for 24 h. (**d**) ChIP analysis of NF-YC9 binding to the *SOC1* regulatory regions in *nf-yc9-1 pNF-YC9:NF-YC9-FLAG* plants described in **c**. Values are mean ± s.d. of three biological replicates. Asterisks indicate significant changes in ChIP-enrichment fold in GA- or PAC-treated samples compared with mock-treated samples (two-tailed Student's *t*-test, $P<0.05$).

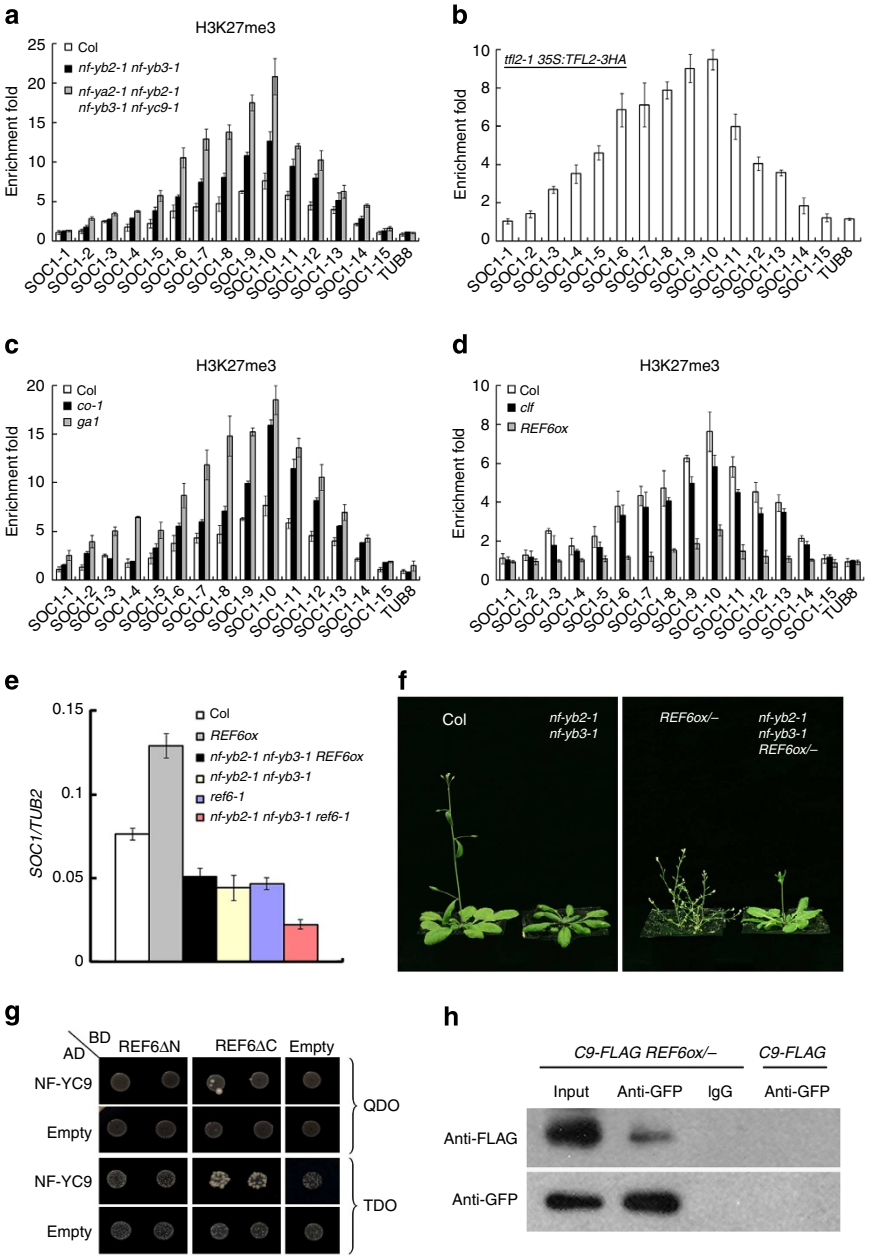

Figure 5 | NF-Y affects H3K27me3 dynamics at *SOC1* and interacts with REF6. (**a**) NF-Y affects H3K27me3 levels at *SOC1*. ChIP analysis of H3K27me3 levels was performed with 9-day-old plants grown under LDs. Values are mean ± s.d. of three biological replicates. (**b**) ChIP analysis of TFL2-3HA binding to the *SOC1* regulatory regions. Nine-day-old *tfl2-1 35S:TFL2-3HA* plants were collected for ChIP analysis. (**c**,**d**) ChIP analysis of H3K27me3 levels at *SOC1* in *co-1* and *ga1* (**c**), or in *clf* and *REF6-YFP-HA* overexpression plants (*REF6ox*) (**d**). Nine-day-old plants were collected for ChIP analysis. (**e**) Quantitative RT–PCR analysis of *SOC1* expression in 9-day-old plants with various genetic backgrounds under LDs. *TUB2* was amplified as an internal control. Values are mean ± s.d. of three biological replicates. (**f**) *nf-yb2-1 nf-yb3-1* partially suppresses early flowering of *REF6ox*. Flowering phenotypes of representative 29-day-old plants with various genetic backgrounds grown under LDs were compared. As *REF6ox* homozygous plants are very tiny and flower extremely early, the phenotypic comparison was made among plants with the *REF6ox* heterozygous background (*REF6ox/ – *). (**g**) Yeast two-hybrid assays show the interaction between NF-YC9 and the N terminus of REF6. Transformed yeast cells were grown on SD-Trp/-Leu/-His (TDO) or SD-Trp/-Leu/-His/-Ade medium (QDO). (**h**) *In vivo* interaction between NF-YC9 and REF6 in *Arabidopsis*. Plant nuclear extracts from 9-day-old *nf-yc9-1 pNF-YC9:NF-YC9-FLAG* and *nf-yc9-1 pNF-YC9:NF-YC9-FLAG REF6ox/ –* seedlings were immunoprecipitated by anti-GFP antibody or preimmune serum (IgG). The co-immunoprecipitated proteins were detected by anti-FLAG or anti-GFP antibody as indicated on the left of each blot. *C9-FLAG*, *nf-yc9-1 pNF-YC9:NF-YC9-FLAG*.

(Fig. 5a) was consistent with decreased expression of *SOC1* in these mutants (Fig. 2a), suggesting that NF-Y subunits might play a redundant role in affecting H3K27me3 levels at *SOC1*. In addition, H3K27me3 levels also greatly increased at *SOC1* in *co-1* and *ga1* (Fig. 5c). These results indicate that the effect of CO and GA signalling on *SOC1* mediated by NF-Y is associated with H3K27me3 levels at *SOC1*.

To further examine the relationship between NF-Y and the H3K27me3 status at *SOC1*, we measured H3K27me3 levels at the native and mutated *pSOC1:GUS* transgene loci in the native and mutated *pSOC1:GUS* plants, respectively (Fig. 3d). H3K27me3 levels were much higher at the mutated locus (Supplementary Fig. 15), indicating that NFYBE bound by NF-Y is involved in mediating H3K27me3 levels at *SOC1*.

NF-Y mediates H3K27me3 demethylation at *SOC1* partly via *REF6*. Because H3K27me3 is deposited by H3K27me3 methyltransferases of the polycomb repressive complex 2 and removed by H3K27 demethylases, we then examined whether NF-Y modulates H3K27me3 dynamics at *SOC1* through its interaction with CURLY LEAF (CLF), a main H3K27me3 methyltransferase, or REF6, a H3K27 demethylase, both of which affect flowering in *Arabidopsis* (Table 1)[46–49].

As both *clf* and *REF6-YFP-HA* overexpression (*REF6ox*) plants exhibit global changes in H3K27me3 levels[46,47], we performed ChIP assays on these two types of plants and found that overexpression of *REF6* dramatically reduced H3K27me3 levels at *SOC1*, whereas there was no significant change in H3K27me3 levels in *clf* (Fig. 5d). Although REF6 was also reported to act as an H3K4me3/H3K36me3 demethylase[50], we did not observe significant changes in H3K4me3/H3K36me3 levels at *SOC1* in both *REF6ox* and *ref6-1* compared with wild-type plants (Supplementary Fig. 16). In agreement with *REF6* role in reducing H3K27me3 levels, *SOC1* was upregulated in *REF6ox* and slightly downregulated in *ref6-1* (Fig. 5e). In contrast, *SOC1* was unexpectedly downregulated in *clf* (Supplementary Fig. 17), which could indirectly result from the effect of *CLF* on *SOC1* upstream regulators, such as *FLOWERING LOCUS C*[46].

Having shown that both NF-Y and REF6 promoted *SOC1* expression through reducing H3K27me3 levels (Fig. 5a,d,e), we crossed *nf-yb2-1 nf-yb3-1* with *REF6ox* and *ref6-1* to investigate whether NF-Y interacts with REF6 to affect *SOC1* expression. Upregulation of *SOC1* in *REF6ox* was attenuated by *nf-yb2-1 nf-yb3-1* (Fig. 5e), which is consistent with the observation that *nf-yb2-1 nf-yb3-1* partially suppressed the extremely early flowering phenotype of *REF6ox* (Fig. 5f, Table 1). Furthermore, *SOC1* expression was lower in *nf-yb2-1 nf-yb3-1 ref6-1* than in *nf-yb2-1 nf-yb3-1* and *ref6-1* (Fig. 5e). Consequently, the late-flowering phenotype of *ref6-1* was enhanced by *nf-yb2-1 nf-yb3-1* (Table 1). These results support that NF-Y partially mediates REF6 effect on *SOC1* expression. As NF-Y did not affect mRNA expression of *REF6* (Supplementary Fig. 18), we then tested the protein interaction between a NF-Y subunit, NF-YC9 and REF6. Yeast two-hybrid assay revealed the interaction between NF-YC9 and the amino terminus of REF6 in yeast (Fig. 5g), and co-immunoprecipitation analysis of *nf-yc9-1 pNF-YC9:NF-YC9-FLAG REF6ox/−* plants confirmed the interaction between NF-YC9 and REF6 in *Arabidopsis* (Fig. 5h). These findings suggest that NF-Y interacts with REF6 to regulate *SOC1* expression. Consistently, reduction of H3K27me3 levels at *SOC1* in *REF6ox* was suppressed by *nf-yb2-1 nf-yb3-1*, while H3K27me3 levels significantly increased in *nf-yb2-1 nf-yb3-1 ref6-1* compared with those in *ref6-1* and *nf-yb2-1 nf-yb3-1* (Fig. 6a).

ChIP assays using a previously established *ref6-1 pREF6:REF6-HA* transgenic line, in which a functional version of *REF6-HA* rescued the flowering defect of *ref6-1* (ref. 47) showed that REF6-6HA was associated with *SOC1*, and that this association was significantly attenuated in *nf-yb2-1 nf-yb3-1* and under SD conditions (Fig. 6b,d), but enhanced by GA treatment (Fig. 6c). These data, together with the observation that overexpression of *REF6* dramatically suppressed late flowering of *co-1* and *ga1* (Fig. 6e, Table 1), substantiate that the interaction between REF6 and NF-Y directly regulates *SOC1* downstream of CO and GA signalling.

Discussion

Combinatorial transcription factors, such as NF-Y complexes, play an essential role in regulating eukaryotic gene expression[51]. Unlike other eukaryotic organisms, the plant lineage has multiple genes that encode each subunit of a heterotrimeric NF-Y complex[32,34]. Individual plant NF-Y subunits have been shown to affect various developmental processes and plant responses to environmental stresses[28–30,52–55]. However, the precise function of complete NF-Y complexes in plants so far remains elusive.

Here we show a NF-Y complex composed of three different types of subunits, NF-YA2, NF-YB2 and NF-YC9, which controls flowering time through directly regulating *SOC1* transcription in response to flowering signals from photoperiod and GA pathways in *Arabidopsis* (Fig. 7). *nf-ya2-1 nf-yb2-1 nf-yb3-1 nf-yc9-1* exhibits much later flowering than *nf-yb2-1 nf-yb3-1* (Table 1), indicating that these NF-Y subunits play redundant roles in promoting flowering. NF-YB and NF-YC subunits interact with CO in the photoperiod pathway as previously reported[28,29], and also with RGA in the GA pathway. Among the NF-Y subunits examined, NF-YC9 serves as a key component that not only mediates the interaction between NF-YA2 and NF-YB2 in the NF-Y heterotrimer (Fig. 1d), but also interacts *in vivo* with CO and RGA (Fig. 1e). A recent study has suggested that plant NF-YC enables translocation of NF-YB to the nucleus, and that the resulting NF-YB/NF-YC heterodimer is required for further recruitment of NF-YA in the final assembly of the heterotrimeric NF-Y complex as shown in mammals[35]. Thus, our finding of NF-YC9 as a common partner of other NF-Y subunits, CO, and RGA implies that NF-YC9 could be a key subunit that coordinates the perception of flowering signals and the assembly of the specific combinatorial NF-Y transcription factor that triggers the downstream regulatory events in response to flowering signals.

Our results suggest that the CO-mediated photoperiod pathway and GA signalling function in parallel in promoting flowering under LDs. The integration of plant responses to these two pathways converges on the NF-Y complex. The genetic data showing the similar late-flowering phenotype of *nf-yb2-1 nf-yb3-1* and *nf-yb2-1 nf-yb3-1 co-1* and complete suppression of early flowering of *SUC2:CO-6HA* by *nf-yb2-1 nf-yb3-1* suggest that CO regulates flowering in a NF-Y-dependent manner. Consistent with the protein interaction between NF-Y and CO, the *SOC1* promoter region associated with NF-Y subunits overlaps with the region bound by CO. Furthermore, the NFYBE in the *SOC1* promoter bound by NF-Y is required for the upregulation of *SOC1* by CO. These observations all support that NF-Y is an important regulator that mediates CO effect on *SOC1* transcription (Fig. 7).

In contrast to CO, RGA in the GA pathway represses *SOC1* transcription. Although RGA interacts with NF-Y, RGA does not directly bind to the *SOC1* promoter. GA treatment degrades RGA, which enhances NF-Y binding to *SOC1*. These results suggest that DELLA proteins, such as RGA, affect *SOC1* expression through preventing NF-Y binding to *SOC1* (Fig. 7). This is substantiated by the observations that the NFYBE in the *SOC1* promoter is indispensable for upregulation of *SOC1* by GA treatment (Fig. 3d,e), and that the flowering response to GA is partially compromised in *nf-ya2-1 nf-yb2-1 nf-yb3-1 nf-yc9-1* (Supplementary Table 1). In addition to *SOC1*, the GA pathway also affects other components of the regulatory network that integrates flowering signals. For example, GA plays spatially distinct regulatory roles in promoting transcription of *FT* and *SPL* genes under LDs[21,56].

It has been demonstrated that NF-Y complexes bind to the CCAAT box, a cis-element present in nearly 25% of eukaryotic promoters, indicating that NF-Y complexes are involved in transcriptional regulation of a considerable number of eukaryotic genes[33,42,57]. Several studies have tested *in vitro* binding sites of plant NF-Y subunits[55,58], but whether these sites are relevant to NF-Y endogenous function is unclear. Another recent study has proposed that NF-Y complexes may recognize a distal CCAAT site at the *FT* promoter based on ChIP assays of *35S:NF-*

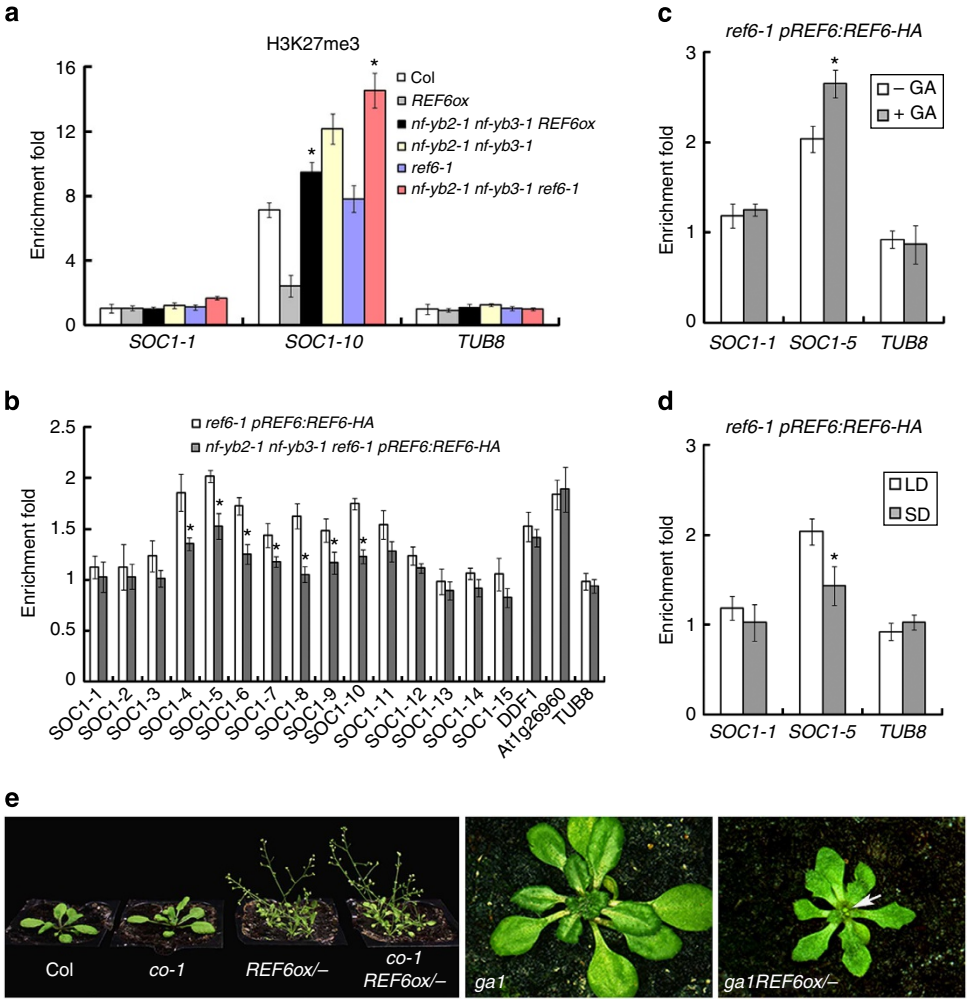

Figure 6 | Interaction between REF6 and NF-Y directly regulates *SOC1* expression downstream of photoperiod and GA pathways. (**a**) ChIP analysis of H3K27me3 levels at *SOC1* in various genetic backgrounds. Nine-day-old plants grown under LDs were collected for ChIP analysis. Values are mean ± s.d. of three biological replicates. Asterisks indicate significant changes in ChIP-enrichment fold in *nf-yb2-1 nf-yb3-1 REF6ox* compared with *REF6ox*, or in *nf-yb2-1 nf-yb3-1 ref6-1* compared with *nf-yb2-1 nf-yb3-1* and *ref6-1* (two-tailed Student's *t*-test, $P<0.05$). (**b**) ChIP analysis of REF6-HA binding to the *SOC1* regulatory regions. Nine-day-old *ref6-1 pREF6:REF6-HA* and *nf-yb2-1 nf-yb3-1 ref6-1 pREF6:REF6-HA* grown under LDs were collected for ChIP analysis. *nf-yb2-1 nf-yb3-1 ref6-1 pREF6:REF6-HA* was generated from a cross between *nf-yb2-1 nf-yb3-1* and *ref6-1 pREF6:REF6-HA*, and exhibited comparable flowering time to *nf-yb2-1 nf-yb3-1* (Table 1). Two known targets, *DDF1* and *At1g26960*, bound by REF6-6HA[47] served as positive controls in ChIP assays. Values are mean ± s.d. of three biological replicates. Asterisks indicate significant changes in ChIP-enrichment fold in *nf-yb2-1 nf-yb3-1 ref6-1 pREF6:REF6-HA* compared with *ref6-1 pREF6:REF6-HA* (two-tailed Student's *t*-test, $P<0.05$). In agreement with NF-Y binding profile (Fig. 3a), REF6-HA is associated with *SOC1-5* with the highest enrichment fold. (**c**,**d**) ChIP analysis of REF6-HA binding to the *SOC1* regulatory regions in response to GA (**c**) and photoperiod (**d**). Nine-day-old *ref6-1 pREF6:REF6-HA* plants grown under LDs treated with 100 μM GA_3 for 24 h (**c**) or grown under short days (SDs) (**d**) were collected for ChIP analysis. Nine-day-old *ref6-1 pREF6:REF6-HA* grown under LDs without GA treatment served as a control for both ChIP analyses shown in (**c**,**d**). Values are mean ± s.d. of three biological replicates. Asterisks indicate significant changes in ChIP-enrichment fold in comparison with respective controls (two-tailed Student's *t*-test, $P<0.05$). (**e**) *REF6ox* suppresses late flowering of *co-1* and *ga1*. The left panel shows representative 27-day-old Col, *co-1*, *REF6ox/–* and *co-1 REF6ox/–* plants, while the middle and right panels show a 29-day-old *ga1* mutant and a 22-day-old *ga1 REF6ox/–* plant, respectively. Arrow indicates floral buds in *ga1 REF6ox/–*.

YB2-YFP/HA plants[59], whereas we were unable to detect binding of NF-YB2-6Myc to *FT* using the *nf-yb2-1 pNF-YB2:NF-YB2-6Myc* tagging line (Supplementary Fig. 9).

We show here that the NF-YA2/NF-YB2/NF-YC9 complex binds to a unique NFYBE, 5′-TTCACAAACACCATT-3′, through NF-YA2. It is noteworthy that this NFYBE does not contain the exact NF-Y consensus binding site, CCAAT, as shown in yeast and animals, implying that the diversity in plant NF-Y subunits may evolve with the divergence of their corresponding *cis*-elements. The *SOC1* genomic region containing the NFYBE demonstrates two unique features that are relevant to regulation of *SOC1* by CO and GA signalling. First, it has been proposed that CO activates *SOC1* through being recruited by a DNA-binding factor to a motif located between nt −372 and −248 in the *SOC1* promoter[18]. This region exactly overlaps with the *SOC1-5* fragment containing the newly identified NFYBE, implying that NF-Y could be the long-sought DNA-binding factor for CO. Furthermore, CO has been shown to bind a CO-responsive element containing a consensus TGTG(N2-3)ATG motif in the *FT* promoter[60]. Notably, there are two similar motifs (TGTGTATG) located 199 bp upstream and 262 bp downstream from the NFYBE in the *SOC1* promoter, respectively. The entire region containing these motifs is associated with CO *in vivo* (Fig. 3a). In concert, these results

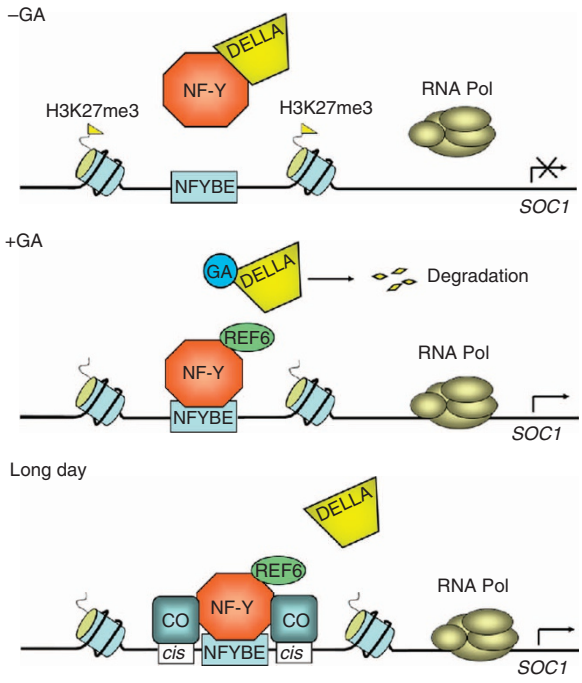

Figure 7 | Photoperiod and GA pathways regulate *SOC1* expression via NF-Y-mediated H3K27me3 demethylation. Without GA, stabilized DELLAs interact with the NF-Y complex and inhibit NF-Y binding to the NFYBE at the *SOC1* locus. This compromises NF-Y-dependent demethylation of H3K27me3, thus repressing *SOC1* expression. Degradation of DELLAs triggered by GA liberates NF-Y to bind to the NFYBE. NF-Y then recruits REF6 to demethylate H3K27me3 at *SOC1*, thus promoting *SOC1* expression. Under LD conditions, stabilized CO protein interacts with NF-Y regardless of the presence of DELLAs. Both of CO and NF-Y bind to the *SOC1* regulatory regions, which facilitates NF-Y-mediated demethylation of H3K27me3 and promotes *SOC1* expression.

suggest that CO and NF-Y interact at the same region centred on the NFYBE to activate *SOC1* transcription.

Second, the forepart of the NFYBE is similar to a GA-responsive *cis*-element (GARE), 5′-TAACAAA/G-3′, which has been identified from an *α-amylase* gene in barley aleurone layers[61]. This element is bound by GAMYB, a GA-inducible transcriptional factor, which activates the *α-amylase* gene expression in aleurone cells[62]. In *Arabidopsis*, the GARE is significantly enriched in the promoters of GA-responsive genes[63]. AtMYB33, a GAMYB protein, has been suggested to promote flowering through binding to a GARE-like element in the *LFY* promoter[64]. Thus, it is tempting to speculate that the interaction between DELLAs and NF-Y may also affect NF-Y interaction with other GARE-binding *trans*-acting partners at the NFYBE, thus mediating the downstream response of GA signalling in plants.

NF-YB and NF-YC subunits have conserved histone fold motifs that resemble H2B and H2A, respectively, both of which, together with H3 and H4, are core histones of the nucleosome, the fundamental unit of chromatin[65]. In yeast and animals, NF-Y could modulate chromatin structure and function through replacement of H2A-H2B and/or covalent modifications of histones, such as methylation and acetylation[33]. One of the most intriguing questions relevant to NF-Y function is how the interaction between NF-Y and other transcriptional regulators mediates spatial and temporal regulation of selected specific loci rather than bulk chromatin.

In this study, we show that a plant NF-Y complex plays an important role in integrating environmental and developmental signals to govern the selection of a specific key regulator to be targeted by a general histone demethylase. NF-Y mediates the effect of photoperiod and GA signalling on *SOC1* expression partly through modulating H3K27me3 demethylation via a H3K27 demethylase REF6. Both CO and RGA interact with NF-Y that directly binds to the NFYBE in the *SOC1* promoter, which in turn mediates REF6 to modulate H3K27me3 levels at *SOC1*. Our findings establish NF-Y as a key complex that orchestrates plant responses to seasonal changes in day length and the endogenous phytohormone GA to mediate epigenetic control of the floral transition in a locus-specific manner. As different combinations of multiple NF-Y subunits may result in the formation of various NF-Y complexes with different intrinsic properties and *trans*-acting partners, this flexibility could allow plants to respond and adapt to various stresses through controlling a large number of specific targets at the molecular level, although they cannot move away from stressful environments.

Methods

Plant materials and growth conditions. *Arabidopsis* plants were grown at 22 °C under LDs (16 h light/8 h dark) or short days (8 h light/16 h dark). The mutants *ga1-3*, *rga-t2*, *gai-t6*, *rgl1-1*, *rgl2-1* and *co-2* are in L*er* background, while all the other mutants are in Col background. *nf-yb2-1* (SALK_025666), *nf-yb3-1* (SALK_062245), *nf-yc9-1* (SALK_058903), *nf-yc4-1* (SALK_032163) and *clf* (SALK_006658) seeds were obtained from the *Arabidopsis* Biological Resource Centre, while *nf-ya2-1* (GK-440G05) and *nf-yc3-2* (GK-051E10) were obtained from the European *Arabidopsis* Stock Centre. Seeds with *ga1-3* or *ga1* background were imbibed in 100 μM GA_3 at 4 °C for 7 days and rinsed thoroughly with water before sowing.

Plasmid construction and plant transformation. To construct *35S:NF-YC9-6HA*, *35S:NF-YC3-6HA* and *35S:NF-YA2-6HA*, the cDNAs encoding NF-YC9, NF-YC3 and NF-YA2 were amplified and cloned into pGreen-35S-6HA, respectively[5]. To construct *pNF-YC9: NF-YC9-FLAG* and *pNF-YB2:NF-YB2-6Myc*, the genomic fragments of *NF-YC9* and *NF-YB2* were amplified and cloned into pHY105-6Myc and pPZPY122-FLAG[26], respectively. The *SUC2* promoter fragment and the cDNA encoding CO were amplified and cloned into pHY105-6HA to obtain *SUC2:CO-6HA*. For the complementation test, a 6.6-kb *SOC1* genomic fragment that includes 2.4 kb of the upstream sequence, 3.5 kb of the transcribed region, and 0.7 kb of the 3′-flanking region was amplified and cloned into pHY105 (ref. 5) to obtain the *gSOC1* construct. Based on the native *gSOC1* and the previously reported *pSOC1:GUS* constructs[5], the derived constructs with the mutated NFYBE were produced using QuikChange II XL-Site-Directed Mutagenesis Kit (Stratagene). Primers used for plasmid construction are listed in Supplementary Table 2. Except for transgenic plants harbouring *pNF-YC9:NF-YC9-FLAG* that were selected on MS medium supplemented with gentamicin, transgenic plants with other constructs were selected by Basta on soil.

Yeast two-hybrid and three-hybrid assays. The coding regions of *NF-YC1*, *NF-YC9*, *NF-YC3*, *NF-YB1*, *NF-YB2*, *NF-YB3*, *NF-YA1*, *NF-YA2*, *CO* and *DELLAs* were amplified and cloned into either pGBKT7 or pGADT7 (Clontech). Yeast two-hybrid assays were performed using the Yeastmaker Yeast Transformation System 2 (Clontech). To screen an *Arabidopsis* cDNA library (CD4-30, from ABRC)[66], the fragment of RGAΔN (residues 200–587) was fused to the GAL4-BD as bait. To analyse the interaction between NF-YC9 and REF6, the carboxy- and N-terminal fragments of REF6 were amplified and cloned into pGBKT7 to obtain *BD-REF6ΔN* and *BD-REF6ΔC*, respectively. To analyse the formation of the trimeric NF-Y complex, the *NF-YC9* coding region was amplified and cloned into pQH05, which was derived from pTH184 with a *HIS3* selection marker. Primers used for generating constructs for yeast two-hybrid and three-hybrid assays are listed in Supplementary Table 2. Yeast AH109 cells were co-transformed with specific bait and prey constructs. For yeast three-hybrid assay, yeast AH109 cells were co-transformed with *AD-NF-YB2/NF-YB3* and *BD-NF-YA1/NF-YA2* in the presence of either *pQH05* or *pQH05-NF-YC9*. All yeast transformants were grown on SD/-Trp/-Leu/-His/-Ade medium for selection or interaction test.

Expression analysis. Total RNA was extracted using the FavorPre Plant Total RNA Mini Kit (Favorgen) and reverse transcribed using the SuperScrip RT–PCR System (Invitrogen). Real-time PCR was performed in triplicates on CFX38 real-time system (Bio-Rad) with the iQ SYBR Green Supermix (Bio-Rad). The relative expression level was calculated as previously reported[5]. Primers used for gene

expression analysis are listed in Supplementary Table 2. GUS staining and quantitative analysis of GUS activity were carried out as previously described[67].

***In vitro* pull-down assay.** To produce GST-tagged proteins, the cDNAs encoding RGA and CO were cloned into pGEX-4T-1 vector (Pharmacia). To produce His-tagged proteins, the cDNAs encoding NF-YC9, NF-YB2 and NF-YA2 were cloned into pQE30 vector (Qiagen). Primers used for these constructs are listed in Supplementary Table 2. These constructs and the empty pGEX-4T-1 and pQE30 vectors were transformed into *E. coli* Rosetta (DE3) (Novagen), and protein expression was induced by IPTG. The soluble His fusion proteins were immobilized onto Ni-NTA agarose beads (30210, Qiagen), while the soluble GST fusion proteins were immobilized onto glutathione sepharose beads (17-0756-01, Amersham Biosciences). For pull-down assays, 2 μg His fusion proteins were incubated with the immobilized GST and GST fusion proteins at 4 °C for 1 h. Proteins retained on the beads were subsequently resolved by SDS–polyacrylamide gel electrophoresis and detected with anti-His antibody (Santa Cruz Biotechnology). Uncropped scans of western blot results are shown in Supplementary Fig. 19.

ChIP assay. Nine-day-old seedlings with various genetic backgrounds were fixed on ice for 45 min in 1% formaldehyde under vacuum. Fixed tissues were homogenized, and chromatin was isolated and sonicated as previously described[5]. The solubilized chromatin was immunoprecipitated by either a specific antibody or mouse IgG (15,381, Sigma) with Protein G PLUS agarose (sc-2002, Santa Cruz Biotechnology). NF-YC9-FLAG, NF-YB2-6Myc, NF-YA2-6HA and CO-6HA were immunoprecipitated by anti-FLAG (A2220, Sigma), anti-Myc (A7470, Sigma) and anti-HA agarose conjugates (A2095, Sigma), respectively. Various histone modifications were detected by anti-H3K27me3 (07-449, Millipore), anti-H3K4me2 (07-030, Millipore), anti-H3K4me3 (07-473, Millipore), anti-H3K36me3 (ab9050, Abcam), anti-H3K9ac (06-942, Millipore), anti-Acetyl-H3 (06-599, Millipore) and anti-Acetyl-H4 antibodies (06-866, Millipore). The co-immunoprecipitated DNA was recovered and analysed by quantitative real-time PCR in triplicates. For ChIP assays of H3K27me3 levels and binding of CO and various NF-Y subunits to *SOC1*, relative fold enrichment was calculated by normalizing the amount of a target DNA fragment against that of a genomic fragment of a reference gene, *ACTIN7* (*At5g09810*), and then by normalizing the value for immunoprecipitation using a specific antibody against that of mouse IgG. The enrichment of a *Tubulin* (*TUB8*; *At5g23860*) genomic fragment was used as a negative control. For ChIP assays of H3ac, H4ac, H3K4me2, H3K4me3, H3K36me3 and H3K9ac levels, *Ta2* transposon (*At4g06488*) served as a reference gene, while the enrichment of a *Cinful-like* (*At4g03770*) genomic fragment was used as a negative control[68].

Co-immunoprecipitation assay. Nine-day-old seedlings with various genetic backgrounds were collected, and nuclear proteins were extracted according to the ChIP protocol but without the tissue fixation step. NF-YC9-FLAG was immunoprecipitated by anti-FLAG agarose conjugate (A2220, Sigma), anti-Myc agarose conjugate (A7470, Sigma), or anti-GFP antibody (A11122, Invitrogen). Proteins bound to the beads were resolved by SDS–polyacrylamide gel electrophoresis and detected by anti-Myc (SAB4700447, Sigma), anti-FLAG (F3165, Sigma), anti-HA (H9658, Sigma), or anti-GFP antibody (A11122, Invitrogen). Uncropped scans of Western blot results are shown in Supplementary Fig. 19.

BiFC analysis. The cDNAs of the proteins tested were cloned into serial pSAT1 vectors containing either N- or C-terminal-enhanced yellow fluorescence protein fragments. The resulting cassettes were further subcloned into a pGreen binary vector HY105 for BiFC analysis as previously published[61].

EMSA. EMSA assay was performed using the LightShift Chemiluminescent EMSA kit (Pierce). The *SOC1-5* fragment or the double-stranded oligonucleotides of the native and mutated NF-YA2 binding element in the *SOC1* promoter with 13 bp flanking sequences at both ends[69] were biotin end labelled and used as probes. Non-labelled probes were used as cold competitors.

References

1. Simpson, G. G. & Dean, C. Flowering–*Arabidopsis*, the rosetta stone of flowering time? *Science* **296,** 285–289 (2002).
2. Lee, H. *et al.* The AGAMOUS-LIKE 20 MADS domain protein integrates floral inductive pathways in *Arabidopsis*. *Genes Dev.* **14,** 2366–2376 (2000).
3. Samach, A. *et al.* Distinct roles of CONSTANS target genes in reproductive development of *Arabidopsis*. *Science* **288,** 1613–1616 (2000).
4. Wang, J. W., Czech, B. & Weigel, D. miR156-regulated SPL transcription factors define an endogenous flowering pathway in *Arabidopsis thaliana*. *Cell* **138,** 738–749 (2009).
5. Liu, C. *et al.* Direct interaction of *AGL24* and *SOC1* integrates flowering signals in *Arabidopsis*. *Development* **135,** 1481–1491 (2008).
6. Putterill, J., Robson, F., Lee, K., Simon, R. & Coupland, G. The *CONSTANS* gene of *Arabidopsis* promotes flowering and encodes a protein showing similarities to zinc finger transcription factors. *Cell* **80,** 847–857 (1995).
7. Suarez-Lopez, P. *et al.* CONSTANS mediates between the circadian clock and the control of flowering in *Arabidopsis*. *Nature* **410,** 1116–1120 (2001).
8. Valverde, F. *et al.* Photoreceptor regulation of CONSTANS protein in photoperiodic flowering. *Science* **303,** 1003–1006 (2004).
9. Kumar, S. V. *et al.* Transcription factor PIF4 controls the thermosensory activation of flowering. *Nature* **484,** 242–245 (2012).
10. Wigge, P. A. *et al.* Integration of spatial and temporal information during floral induction in *Arabidopsis*. *Science* **309,** 1056–1059 (2005).
11. An, H. *et al.* CONSTANS acts in the phloem to regulate a systemic signal that induces photoperiodic flowering of *Arabidopsis*. *Development* **131,** 3615–3626 (2004).
12. Corbesier, L. *et al.* FT protein movement contributes to long-distance signaling in floral induction of *Arabidopsis*. *Science* **316,** 1030–1033 (2007).
13. Liu, L. *et al.* FTIP1 is an essential regulator required for florigen transport. *PLoS Biol.* **10,** e1001313 (2012).
14. Li, D. *et al.* A repressor complex governs the integration of flowering signals in *Arabidopsis*. *Dev. Cell* **15,** 110–120 (2008).
15. Moon, J. *et al.* The *SOC1* MADS-box gene integrates vernalization and gibberellin signals for flowering in *Arabidopsis*. *Plant J.* **35,** 613–623 (2003).
16. Shen, L., Kang, Y. G., Liu, L. & Yu, H. The J-domain protein J3 mediates the integration of flowering signals in *Arabidopsis*. *Plant Cell* **23,** 499–514 (2011).
17. Yoo, S. K. *et al.* CONSTANS activates *SUPPRESSOR OF OVEREXPRESSION OF CONSTANS 1* through FLOWERING LOCUS T to promote flowering in *Arabidopsis*. *Plant Physiol.* **139,** 770–778 (2005).
18. Hepworth, S. R., Valverde, F., Ravenscroft, D., Mouradov, A. & Coupland, G. Antagonistic regulation of flowering-time gene *SOC1* by CONSTANS and FLC via separate promoter motifs. *EMBO J.* **21,** 4327–4337 (2002).
19. Wilson, R. N., Heckman, J. W. & Somerville, C. R. Gibberellin is required for flowering in *Arabidopsis thaliana* under short days. *Plant Physiol.* **100,** 403–408 (1992).
20. Reeves, P. H. & Coupland, G. Analysis of flowering time control in *Arabidopsis* by comparison of double and triple mutants. *Plant Physiol.* **126,** 1085–1091 (2001).
21. Porri, A., Torti, S., Romera-Branchat, M. & Coupland, G. Spatially distinct regulatory roles for gibberellins in the promotion of flowering of *Arabidopsis* under long photoperiods. *Development* **139,** 2198–2209 (2012).
22. Dill, A. & Sun, T. Synergistic derepression of gibberellin signaling by removing RGA and GAI function in *Arabidopsis thaliana*. *Genetics* **159,** 777–785 (2001).
23. Fu, X. *et al.* The *Arabidopsis* mutant *sleepy1 gar2-1* protein promotes plant growth by increasing the affinity of the SCFSLY1 E3 ubiquitin ligase for DELLA protein substrates. *Plant Cell* **16,** 1406–1418 (2004).
24. de Lucas, M. *et al.* A molecular framework for light and gibberellin control of cell elongation. *Nature* **451,** 480–484 (2008).
25. Feng, S. *et al.* Coordinated regulation of *Arabidopsis thaliana* development by light and gibberellins. *Nature* **451,** 475–479 (2008).
26. Hou, X., Lee, L. Y., Xia, K., Yan, Y. & Yu, H. DELLAs modulate jasmonate signaling via competitive binding to JAZs. *Dev. Cell* **19,** 884–894 (2010).
27. Yu, S. *et al.* Gibberellin regulates the *Arabidopsis* floral transition through miR156-targeted SQUAMOSA PROMOTER BINDING-LIKE transcription factors. *Plant Cell* **24,** 3320–3332 (2012).
28. Kumimoto, R. W., Zhang, Y., Siefers, N. & Holt, B. F. NF-YC3, NF-YC4 and NF-YC9 are required for CONSTANS-mediated, photoperiod-dependent flowering in Arabidopsis thaliana. *Plant J.* **63,** 379–391 (2010).
29. Wenkel, S. *et al.* CONSTANS and the CCAAT box binding complex share a functionally important domain and interact to regulate flowering of *Arabidopsis*. *Plant Cell* **18,** 2971–2984 (2006).
30. Kumimoto, R. W. *et al.* The Nuclear Factor Y subunits NF-YB2 and NF-YB3 play additive roles in the promotion of flowering by inductive long-day photoperiods in *Arabidopsis*. *Planta* **228,** 709–723 (2008).
31. Cai, X. N. *et al.* A putative CCAAT-binding transcription factor is a regulator of flowering timing in *Arabidopsis*. *Plant Physiol.* **145,** 98–105 (2007).
32. Gusmaroli, G., Tonelli, C. & Mantovani, R. Regulation of novel members of the *Arabidopsis thaliana* CCAAT-binding nuclear factor Y subunits. *Gene* **283,** 41–48 (2002).
33. Dolfini, D., Gatta, R. & Mantovani, R. NF-Y and the transcriptional activation of CCAAT promoters. *Crit. Rev. Biochem. Mol. Biol.* **47,** 29–49 (2012).
34. Siefers, N. *et al.* Tissue-specific expression patterns of *Arabidopsis* NF-Y transcription factors suggest potential for extensive combinatorial complexity. *Plant Physiol.* **149,** 625–641 (2009).
35. Hackenberg, D. *et al.* Studies on differential nuclear translocation mechanism and assembly of the three subunits of the *Arabidopsis thaliana* transcription factor NF-Y. *Mol. Plant* **5,** 876–888 (2012).
36. Yu, H. *et al.* Floral homeotic genes are targets of gibberellin signaling in flower development. *Proc. Natl Acad. Sci. USA* **101,** 7827–7832 (2004).

37. Lee, L. Y. *et al.* *STUNTED* mediates the control of cell proliferation by GA in *Arabidopsis*. *Development* **139,** 1568–1576 (2012).
38. Onouchi, H., Igeno, M. I., Perilleux, C., Graves, K. & Coupland, G. Mutagenesis of plants overexpressing *CONSTANS* demonstrates novel interactions among *Arabidopsis* flowering-time genes. *Plant Cell* **12,** 885–900 (2000).
39. Xing, Y., Fikes, J. D. & Guarente, L. Mutations in yeast *HAP2/HAP3* define a hybrid CCAAT box binding domain. *EMBO J.* **12,** 4647–4655 (1993).
40. Brazda, V., Laister, R. C., Jagelska, E. B. & Arrowsmith, C. Cruciform structures are a common DNA feature important for regulating biological processes. *BMC Mol. Biol.* **12,** 33 (2011).
41. Gatta, R. & Mantovani, R. NF-Y affects histone acetylation and H2A.Z deposition in cell cycle promoters. *Epigenetics* **6,** 526–534 (2011).
42. Donati, G. *et al.* An NF-Y-dependent switch of positive and negative histone methyl marks on CCAAT Promoters. *PLoS ONE* **3,** e2066 (2008).
43. Gatta, R. & Mantovani, R. NF-Y substitutes H2A-H2B on active cell-cycle promoters: recruitment of CoREST-KDM1 and fine-tuning of H3 methylations. *Nucleic Acids Res.* **36,** 6592–6607 (2008).
44. Zhang, X. *et al.* The *Arabidopsis* LHP1 protein colocalizes with histone H3 Lys27 trimethylation. *Nat. Struct. Mol. Biol.* **14,** 869–871 (2007).
45. Liu, C., Xi, W., Shen, L., Tan, C. & Yu, H. Regulation of floral patterning by flowering time genes. *Dev. Cell* **16,** 711–722 (2009).
46. Jiang, D. H., Wang, Y. Q., Wang, Y. Z. & He, Y. H. Repression of *FLOWERING LOCUS C* and *FLOWERING LOCUS T* by the *Arabidopsis* Polycomb Repressive Complex 2 components. *PLoS ONE* **3,** e3404 (2008).
47. Lu, F. L., Cui, X., Zhang, S. B., Jenuwein, T. & Cao, X. F. *Arabidopsis* REF6 is a histone H3 lysine 27 demethylase. *Nat. Genet.* **43,** 715–719 (2011).
48. Chanvivattana, Y. *et al.* Interaction of Polycomb-group proteins controlling flowering in *Arabidopsis*. *Development* **131,** 5263–5276 (2004).
49. Hennig, L. & Derkacheva, M. Diversity of Polycomb group complexes in plants: same rules, different players? *Trends Genet.* **25,** 414–423 (2009).
50. Ko, J. H. *et al.* Growth habit determination by the balance of histone methylation activities in Arabidopsis. *EMBO J.* **29,** 3208–3215 (2010).
51. Singh, K. B. Transcriptional regulation in plants: the importance of combinatorial control. *Plant Physiol.* **118,** 1111–1120 (1998).
52. Lotan, T. *et al.* *Arabidopsis* LEAFY COTYLEDON1 is sufficient to induce embryo development in vegetative cells. *Cell* **93,** 1195–1205 (1998).
53. Nelson, D. E. *et al.* Plant nuclear factor Y (NF-Y) B subunits confer drought tolerance and lead to improved corn yields on water-limited acres. *Proc. Natl Acad. Sci. USA* **104,** 16450–16455 (2007).
54. Li, W. X. *et al.* The *Arabidopsis* NFYA5 transcription factor is regulated transcriptionally and posttranscriptionally to promote drought resistance. *Plant Cell* **20,** 2238–2251 (2008).
55. Liu, J. X. & Howell, S. H. bZIP28 and NF-Y Transcription factors are activated by ER stress and assemble into a transcriptional complex to regulate stress response genes in *Arabidopsis*. *Plant Cell* **22,** 782–796 (2010).
56. Galvao, V. C., Horrer, D., Kuttner, F. & Schmid, M. Spatial control of flowering by DELLA proteins in *Arabidopsis thaliana*. *Development* **139,** 4072–4082 (2012).
57. Mantovani, R. The molecular biology of the CCAAT-binding factor NF-Y. *Gene* **239,** 15–27 (1999).
58. Kusnetsov, V., Landsberger, M., Meurer, J. & Oelmuller, R. The assembly of the CAAT-box binding complex at a photosynthesis gene promoter is regulated by light, cytokinin, and the stage of the plastids. *J. Biol. Chem.* **274,** 36009–36014 (1999).
59. Cao, S. *et al.* A distal *CCAAT*/NUCLEAR FACTOR Y complex promotes chromatin looping at the *FLOWERING LOCUS T* promoter and regulates the timing of flowering in *Arabidopsis*. *Plant Cell* **26,** 1009–1017 (2014).
60. Tiwari, S. B. *et al.* The flowering time regulator CONSTANS is recruited to the *FLOWERING LOCUS T* promoter via a unique cis-element. *New Phytol.* **187,** 57–66 (2010).
61. Skriver, K., Olsen, F. L., Rogers, J. C. & Mundy, J. cis-acting DNA elements responsive to gibberellin and its antagonist abscisic acid. *Proc. Natl Acad. Sci. USA* **88,** 7266–7270 (1991).
62. Gubler, F., Kalla, R., Roberts, J. K. & Jacobsen, J. V. Gibberellin-regulated expression of a myb gene in barley aleurone cells: evidence for Myb transactivation of a high-pI alpha-amylase gene promoter. *Plant Cell* **7,** 1879–1891 (1995).
63. Bastian, R. *et al.* Gibberellic acid and cGMP-dependent transcriptional regulation in *Arabidopsis thaliana*. *Plant Signal. Behav.* **5,** 224–232 (2010).
64. Gocal, G. F. W. *et al.* *GAMYB*-like genes, flowering, and gibberellin signaling in *Arabidopsis*. *Plant Physiol.* **127,** 1682–1693 (2001).
65. Luger, K., Mader, A. W., Richmond, R. K., Sargent, D. F. & Richmond, T. J. Crystal structure of the nucleosome core particle at 2.8A resolution. *Nature* **389,** 251–260 (1997).
66. Fan, H. Y., Hu, Y., Tudor, M. & Ma, H. Specific interactions between the K domains of AG and AGLs, members of the MADS domain family of DNA binding proteins. *Plant J.* **12,** 999–1010 (1997).
67. Jefferson, R. A., Kavanagh, T. A. & Bevan, M. W. GUS fusions: beta-glucuronidase as a sensitive and versatile gene fusion marker in higher plants. *EMBO J.* **6,** 3901–3907 (1987).
68. Schonrock, N. *et al.* Polycomb-group proteins repress the floral activator *AGL19* in the *FLC*-independent vernalization pathway. *Genes Dev.* **20,** 1667–1678 (2006).
69. Tang, W. & Perry, S. E. Binding site selection for the plant MADS domain protein AGL15: an in vitro and in vivo study. *J. Biol. Chem.* **278,** 28154–28159 (2003).

Acknowledgements

We thank X.F. Cao for providing *ref6-1*, *REF6ox* and *ref6-1 pREF6:REF6-HA* seeds, the Arabidopsis Biological Resource Centre for *nf-yb2-1*, *nf-yb3-1*, *nf-yc9-1*, and *nf-yc4-1* seeds, and the European Arabidopsis Stock Centre for *nf-ya2-1* and *nf-yc3-2* seeds. This work was supported by Academic Research Funds (MOE2011-T2-2-008 and R-154-000-506-112) from the Ministry of Education-Singapore, the Singapore National Research Foundation under its Competitive Research Programme (NRF2010NRF-CRP002-018), and the intramural resource support from National University of Singapore and Temasek Life Sciences Laboratory.

Author contributions

X.H. and H.Y. conceived and designed the research. X.H., J.Z., C.L., L.L., and L.S. performed the experiments. X.H., J.Z. and H.Y. analysed the data. X.H. and H.Y. wrote the paper.

Additional information

Supplementary Information accompanies this paper at http://www.nature.com/naturecommunications

Competing financial interests: The authors declare no competing financial interests.

Reprints and permission information is available online at http://npg.nature.com/reprintsandpermissions/

How to cite this article: Hou, X. *et al.* Nuclear factor Y-mediated H3K27me3 demethylation of the *SOC1* locus orchestrates flowering responses of *Arabidopsis*. *Nat. Commun.* 5:4601 doi: 10.1038/ncomms5601 (2014).